**Uncertainty Quantification in Internal Dose Calculations for Seven Selected Radiopharmaceuticals**

Vladimir Spielmann, Wei Bo Li, Maria Zankl, Uwe Oeh, Christoph Hoeschen

Research Unit Medical Radiation Physics and Diagnostics, Helmholtz Zentrum München - German Research Center for Environmental Health, Neuherberg, Germany

**Concise and informative title**

Uncertainty of absorbed Dose

**Corresponding authors**

Vladimir Spielmann

Research Unit Medical Radiation Physics and Diagnostics

Helmholtz Zentrum München - German Research Center for Environmental Health

Neuherberg, Germany

vladimir.spielmann@helmholtz-muenchen.de

Phone: +49 (0) 89 3187 2639

Fax: +49 (0) 89 3187 3846

Wei Bo Li

Research Unit Medical Radiation Physics and Diagnostics

Helmholtz Zentrum München - German Research Center for Environmental Health

Neuherberg, Germany

wli@helmholtz-muenchen.de

Phone: +49 (0) 89 3187 3314

Fax: +49 (0) 89 3187 3846

**Abstract**

Dose coefficients of radiopharmaceuticals have been published by the International Commission on Radiological Protection (ICRP) and the Medical Internal Radiation Dose (MIRD) Committee, but without information concerning uncertainties. The uncertainty information of dose coefficients is important, for example, to compare alternative diagnostic methods and choose the method that causes the lowest patient exposure with appropriate and comparable diagnostic quality. For the study presented here, an uncertainty analysis method was developed and used to calculate the uncertainty of the internal doses of seven common radiopharmaceuticals. **Methods:** On the basis of the generalized schema of dose calculation recommended by ICRP and the MIRD Committee, an analysis based on propagation of uncertainty was developed and applied for seven radiopharmaceuticals. The method takes into account the uncertainties contributed from pharmacokinetic models and the so-called S values derived from several voxel computational phantoms previously developed at Helmholtz Zentrum München. Random and Latin hypercube sampling techniques were used to sample parameters of pharmacokinetic models and S values, and the uncertainties of absorbed doses and effective doses were calculated. **Results:** The uncertainty factors (square root of ratio between 97.5th and 2.5th percentiles) for organ absorbed doses are in the range of 1.1 to 3.3. Uncertainty values of effective doses are lower in comparison to absorbed doses, the maximum value being approximately 1.4. The ICRP reference values showed a deviation comparable to the effective dose calculated in this study. **Conclusion:** A general statistical method was developed for calculating the uncertainty of absorbed doses and effective doses for seven radiopharmaceuticals. The dose uncertainties can be used to further identify the most important parameters in the dose calculation and provide reliable dose coefficients for risk analysis of the patients in nuclear medicine.

**Key Words:** uncertainty quantification; internal dosimetry; pharmacokinetic model; voxel phantom; nuclear medicine.

## INTRODUCTION

The absorbed and effective dose coefficients (DCs) to the patients from administered radiopharmaceuticals are usually calculated according to the generalized schema recommended by the ICRP and the MIRD of the Society of Nuclear Medicine and Molecular Imaging (SNMMI) (*1-3*). In these calculations, the mathematical models (*4*) for the time-dependent activity curves in organs and tissues (pharmacokinetic models), and the mathematical and digital representations of the human body (now voxel phantoms) (*5*) are initially evaluated. Because of the uncertainties in the image acquisition chains and the variability of the patients, the image-based kinetic models and the reference human phantoms used for the estimation of absorbed doses to patients are subject to large sources of uncertainty (*6-8*). Hence, for an individual patient, the resulting dose coefficients are uncertain.

Generally, the radiation doses to patients are reported without associated uncertainty and this information is important, for example, to compare alternative diagnostic methods and choose the method that causes the lowest patient exposure with appropriate and comparable diagnostic quality. Furthermore, the uncertainty of internal dose is generally greater than that of external dose, for example in external beam radiation therapy. The calculated internal dose is needed for a medical radiation risk analysis for patients.

In this study, an uncertainty analysis method, based on the propagation of uncertainty, was set up to analyze the two main sources of uncertainties in internal dose calculation for radiopharmaceuticals, namely, the image-based pharmacokinetic model parameters and the S values derived from different voxel phantoms. This practical method was applied to assess the uncertainty of DCs of seven common used radiopharmaceuticals. The uncertainty factors (UF, defined as the square root of ratio between 97.5th and 2.5th percentiles) for absorbed dose coefficients are in the range between 1.1 and 3.3; for effective dose the UFs are lower in comparison to absorbed dose, the maximum value being about 1.4. The uncertainty of DCs can be used for risk analysis of patients undergoing diagnostic nuclear medicine procedures.

## MATERIALS AND METHODS

### Radiopharmaceuticals

In this study, the uncertainty of absorbed dose coefficient and effective dose coefficient are calculated for the following radiopharmaceuticals: $^{18}$F-FDG ($^{18}$F-fluorodeoxyglucose), $^{99m}$Tc-pertechnetate, $^{99m}$Tc-phosphonate, $^{99m}$Tc-sestamibi, $^{99m}$Tc-tetrofosmin, $^{99m}$Tc-MAA (Macroaggregated Albumin) and $^{201}$Tl-chloride.

### Calculation of Dose Coefficients

In this work, the generalized schema for radiopharmaceutical dosimetry published by the MIRD Committee and ICRP (*3*) was used for calculating the internal doses. The absorbed dose $D(r_T, T_D)$ in the target organ $r_T$ is determined by:

$$D(r_T, T_D) = \sum_{r_S} \tilde{A}(r_S, T_D) S(r_T \leftarrow r_S) + \tilde{A}(REM) \left[ \left( M_{TB} S(r_T \leftarrow TB) - \sum_{r_S} M_{r_S} S(r_T \leftarrow r_S) \right) / M_{REM} \right] \quad \text{(Eq. 1)}$$

where $\tilde{A}(r_S, T_D)$ is the time-integrated activity in a source organ or region $r_S$ over the integration period $T_D$, where $T_D$ is commonly taken to be infinity (*3*); $S(r_T \leftarrow r_S)$ is the radionuclide-specific quantity representing the mean absorbed dose to target tissue $r_T$ per unit activity in source tissue $r_S$, the so-called S value; $M_{TB}$ and $M_{REM}$ are the organ mass (g) of the total body (TB) without contents of walled organs and the organ mass (g) in the remainder tissues (REM), respectively, with $M_{REM} = M_{TB} - \sum M_{r_S}$.

The ICRP and the MIRD Committee defined the effective dose *E* for a reference person by averaging the equivalent doses of female and male (*9*). However, the objective of this study is to estimate the uncertainty of effective dose, the biokinetic data of the seven radiopharmaceuticals were evaluated from the literature without gender identification and the S values were derived from six male phantoms and one female phantom. Therefore, the uncertainty of effective dose is calculated according to the following formula (*10*):

$$E = \sum_T w_T H(r_T, T_D) \quad \text{(Eq. 2)}$$

where $w_T$ is a tissue-weighting factor for the target tissue $r_T$, and $H(r_T, T_D)$ is the committed equivalent dose. The tissue-weighting factors $w_T$ published by ICRP (*9*) were applied and the uncertainty of factors $w_T$ is not taken into account in this study, which is related to risk analysis. In addition, the difference between the dose coefficients of female and male is calculated by using the mathematical and voxel phantoms, respectively (see Table 2).

To quantitatively determine the uncertainties of the dose coefficients (absorbed dose per administered activity), uncertainties of the S values and the time-integrated activity $\tilde{A}(r_S, T_D)$ are evaluated first.

**Determination of the Uncertainty of Time-Integrated Activity**

The time-integrated activity of an administered radiopharmaceutical in a source organ is calculated by solving a system of ordinary linear differential equations with transfer rates $\lambda_{ij}$ as described in (*4*):

$$\frac{dq_i(t)}{dt} = \dot{I}(t) - \sum_{j=0, j\neq i}^{n} \lambda_{ji} q_i(t) - \lambda_p q_i(t) + \sum_{j=1, j\neq i}^{n} \lambda_{ij} q_j(t) \quad \text{(Eq. 3)}$$

where $q_i(t)[Bq]$ is activity of the radioactive substance in compartment $i$ at the time $t$; $\lambda_{ij}[d^{-1}]$ is transfer rate of substance transferred from $j$ to $i$; $\lambda_{ji}$ is the transfer rate from compartment $i$ *to* $j$; $\lambda_{0i}$ is loss rate to outside of the system; $\dot{I}(t)[Bq \cdot d^{-1}]$ is the rate of input from outside of the system; and $\lambda_p$ is the radioactive decay constant. According to (*3*), the time-integrated activity is calculated by $\tilde{A} = \int_0^{T_D} q(t)\, dt$. The MIRD Committee has reported such compartmental models and their corresponding model parameters (transfer rates) for some radiopharmaceuticals.

If the transfer rates are expressed by fraction and half-life, the solution for the above differential equation (Eq. 3) can be obtained. The time-integrated activity can be written as following (*1*):

$$\frac{\tilde{A}_s}{A_0} = F_s \sum_{j=n+1}^{n+m} a_j \sum_{i=1}^{n} [a_i \frac{T_i}{T_i - T_j} (\frac{T_{i,eff}}{\ln(2)} - \frac{T_{j,eff}}{\ln(2)})] \quad \text{(Eq. 4)}$$

where $A_0$ is the administered activity, $F_s$ is the fractional distribution to organ S, $a_i$ is a fraction of $F_s$ eliminated with a biological half-life $T_i$, $a_j$ is the fraction of $F_s$ taken up with a biological half-life $T_j$. Both $a_i$ and $a_j$ follow: $\sum a_i = 1$ and $\sum a_j = 1$. $T_{i,eff}$ and $T_{j,eff}$ are the elimination and uptake effective half-lives, respectively. ICRP applied such mathematical models for many commonly used radiopharmaceuticals and tabulated the corresponding model parameters in its publications (*1,11,12*). In contrast to the MIRD schema, the time-integrated activity can be calculated here explicitly.

The time-integrated activity $\tilde{A}_s$ is a function of parameters $F_s, a_i, a_j, T_i, T_j$ (ICRP analytical method) or parameter $\lambda$ (MIRD compartmental method). To calculate the uncertainty of the $\tilde{A}_s$, the Latin hypercube sampling (LHS) technique (*13*) was used for sampling the parameters in the function. The range between the minimum and maximum values of each parameter is divided into 500 intervals on the basis of equal probability. One value from each interval is selected at random with respect to the probability density in the interval. The 500 values thus obtained for the first parameter are paired in a random manner (equally likely combinations) with the 500 values of the second parameter. These 500 pairs are combined in a random manner with the 500 values of the third parameter to form 500 triples and so forth until 500 k-tuples are formed. In this manner one get an n x k matrix of input where the $i^{th}$ row contains values of each of the k input variables to be used on the $i^{th}$ run (n=500 runs) of the computer model.

To illustrate the MIRD compartmental-model approach, the model structure, the mean values and the standard deviations of the model parameters for $^{18}$F-FDG were taken from Hays et al. (*14*). The minimum and maximum values and the type of the distribution of the model parameters for the LHS sampling were taken from Li et al. (*15*). The FDG compartmental model is depicted in figure 1. For the other six radiopharmaceuticals, based on a normal distribution and a confidence interval of 95%, the minimum and maximum values were calculated as following:

$$Min = \mu - 1.96\sigma$$

$$Max = \mu + 1.96\sigma \quad \text{(Eq. 5)}$$

For the negative values, which occurred in some parameters, a lognormal distribution was assumed. The minimum and maximum values were then recalculated based on the lognormal distribution.

$$\mu^* = \frac{\mu}{\sqrt{1 + \left(\frac{\sigma}{\mu}\right)^2}}$$

$$\sigma^* = \exp\left(\sqrt{\log\left(1 + \left(\frac{\sigma}{\mu}\right)^2\right)}\right) \quad \text{(Eq. 6)}$$

After the geometric mean $\mu^*$ and the geometric standard deviation $\sigma^*$ (*16*) were determined, the minimum and maximum values (97.5$^{th}$ and 2.5$^{th}$ percentiles of the lognormal distribution) were calculated with a confidence interval of 95%:

$$Min = \mu^*/(\sigma^*)^{1.96}$$

$$Max = \mu^* \times (\sigma^*)^{1.96} \quad \text{(Eq. 7)}$$

The mean values of the model parameters for $^{18}$F-FDG and $^{201}$Tl-chloride, in accordance with the ICRP analytical method, were taken from ICRP Publication 106 (*12*), for $^{99m}$Tc-pertechnetate, $^{99m}$Tc-phosphonate and $^{99m}$Tc-MAA from ICRP Publication 53 (*1*), and for $^{99m}$Tc-sestamibi and $^{99m}$Tc-tetrofosmin from ICRP Publication 80 (*11*). To calculate the uncertainty of the model parameter, a normal distribution with a coefficient of variation (CV) of 0.2 was assumed. Some parameters for the source organs, marked with a dagger (Supplemental Tables 2-8), were not specified; however, the time-integrated activity was indicated.

For $^{18}$F-FDG, the uncertainties of the time-integrated activity were calculated by both MIRD and ICRP models. For the remaining six radiopharmaceuticals, the calculations were performed solely by the ICRP method because there is no proposed compartmental model published by the MIRD Committee.

**Determination of Uncertainty of S Values**

The S values were calculated by the specific absorbed fraction values (SAF values), the energy and yield of emitting radiation. The SAF values are the fraction of radiation *R* of

energy *E* emitted within the source region that is absorbed per unit mass in the target region. In our laboratory, the SAF values for seven different phantoms (Table 1) were calculated by applying the Monte Carlo radiation transport simulation technique (*17*). The decay energies and yields, which were taken from the ICRP Publication 107 (*18*), are assumed to be constant in the present uncertainty analysis. Therefore, the uncertainty of the S values is the fractional uncertainty of the SAF values. The standard deviation and mean values were determined from the SAF values of the seven phantoms. For lognormal distributions, the geometric mean and the geometric standard deviation were calculated from which the minimum and maximum values for the SAFs were determined.

The SAF values of electrons for some walled organs were not simulated. For SAF values of electrons with energies less than 100 keV, the following approximations have been made (*19*):

$$\Phi(r_T \leftarrow r_S) = \begin{cases} 1/\mathrm{M_T} & \text{for } r_T = r_S \\ 0 & \text{for } r_T \neq r_S \\ 0.5/\mathrm{M_c} & \text{for } r_T = \text{wall}, r_S = \text{contents of walled organ} \\ 1/\mathrm{M_{TB}} & \text{for } r_S = \text{Total body} \end{cases} \quad \text{(Eq. 8)}$$

where $r_T$ is target region, $r_S$ source region, TB total body, $M_T$ and $M_{TB}$ masses of the target regions and of the total body, respectively, and $\Phi(r_T \leftarrow r_S)$ is the specific absorbed fraction. The minimum and maximum values required for the LHS method were calculated according to the same principle as in the determination of the uncertainties of the model parameters.

A computer program called “DoseU”, written in C#, was developed at the Helmholtz Zentrum München for calculating the uncertainty of the absorbed dose and effective dose coefficients according to Eq. 1 and Eq. 2. As input, 500 sample values of the k parameters of time-integrated activity and S values were generated, and were entered in the computer code “DoseU”. As output, 500 values of absorbed and effective dose coefficients were calculated that were further used for calculating the statistics, for example, 2.5$^{th}$, 25$^{th}$, 75$^{th}$ and 97.5$^{th}$ percentiles, the mean values and standard deviation of the dose coefficients.

187 To demonstrate the deviations in the calculation of dose coefficients with the same
188 time-integrated activities and different phantoms, dose coefficients calculated using voxel
189 phantoms (*17*) and mathematical phantoms (*20*) were compared.

**RESULTS**

The uncertainty of the model parameter for $^{18}$F-FDG, expressed in maximum and minimum values, and the distribution type required for sampling are summarized in the Supplemental Tables 1 and 2. The data for the rest of the radiopharmaceuticals, according to the ICRP analytical method, can be found in the Supplemental Tables 3-8.

For a quantitative description of uncertainty, the uncertainty factor (UF) (*21*) was used. The uncertainty-associated quantity can be expressed in terms of lower and upper bounds, A and B, respectively. The UF for a confidence interval of 95 % is defined as the square root of ratio between 97.5th (B) and 2.5th (A) percentiles. The uncertainty factors for the time-integrated activity varied generally from 1.0 to 2.0. The calculated minimum and maximum values and the type of distribution for the S values are not listed here for reasons of space.

The uncertainties of the dose coefficients are presented in figures 2-5 (logarithmic representation) in the form of boxplots. The boundary line between the two colors of the box reflects the median value. The lower and the upper edge of the box represent, respectively, the 25$^{th}$ and 75$^{th}$ percentile; within the box are the 50$^{th}$ percentiles of all values. The upper and lower end of the whiskers shows the 2.5$^{th}$ and 97.5$^{th}$ percentile, respectively.

For $^{18}$F-FDG, the uncertainty of the dose coefficients, according to the MIRD calculation, varies from 1.2 to 1.7; the large coefficient of variation of the S value (liver-to-UB wall, 29%) leads to the larger UF in UB wall of 1.9. According to the ICRP calculation, the UF ranges from 1.1 to 1.9, especially for brain with a greater UF of 1.5 and UB wall a UF of 1.9. For $^{99m}$Tc-pertechnetate, the UF varies from 1.1 to 1.5, for $^{99m}$Tc-phosphonate from 1.2 to 2.4; the large UF of 2.4 in the brain with $^{99m}$Tc-phosphonate is due to the large geometric standard deviations of the S values of bone-to-brain (2.92) and UB cont-to-brain (2.4). The UFs for $^{99m}$Tc-sestamibi are from 1.1 to 1.6, and for $^{99m}$Tc-tetrofosmin from 1.1 to 1.7. For $^{99m}$Tc-MAA, the UF varies from 1.2 to 2.4, particularly for thymus with a greater UF of 2.4; the large UF of 2.4 in the thymus with $^{99m}$Tc-MAA is due to the large coefficient of variation of the S values of liver-to-thymus (25%) and kidney-to-thymus (28%). Finally,

the UF of $^{201}$Tl-chloride varies from 1.3 to 3.3, with greater uncertainties for lungs (UF = 2.8) and kidneys (UF = 3.3); the very large UF of 3.3 in the kidneys with $^{201}$Tl-chloride is due to the large geometric standard deviations of the S values of bone-to-kidney (2.9) and kidney-to-kidney (3.2), respectively.

The uncertainties of effective dose coefficients are presented in figure 6. The uncertainty factor varies from 1.1 ($^{99m}$Tc-sestamibi) to 1.4 ($^{201}$Tl-chloride). For comparison, the dose coefficients and deviations of $^{18}$F-FDG between the two different types of phantoms are shown in table 2.

## DISCUSSION

The uncertainties in the absorbed dose can mainly be attributed to the uncertainties in the time-integrated activity which is associated with the pharmacokinetic model parameters and the uncertainties of the S values which were derived from the voxel phantoms. For model parameters for there was insufficient information upon which to base an estimate of the uncertainty, we assumed a coefficient of variation of 20%. The mean energy of electrons was used in the calculation of the S values from the SAF values.

The mean values of the dose coefficients calculated in the present work were compared with the values reported by other investigators to show the development of the internal dose calculation and the advanced imaging technology in nuclear medicine.

For $^{18}$F-FDG**,** dose coefficients were reported by ICRP (*1,11,12*), MIRD Committee (*22*), and many other groups (*23-29*). A strong variation of absorbed doses in some target organs was shown. For example, for lungs our calculated value of 0.0208 mGy MBq$^{-1}$ is compared to 0.0046 mGy MBq$^{-1}$ reported by Khamwan et al. (29) and 0.094 mGy MBq$^{-1}$ by Mejia et al. (23); for spleen, our value of 0.0122 mGy MBq$^{-1}$ is compared to the value of 0.05 mGy MBq$^{-1}$ by Reivich et al. (25) and 0.04 mGy MBq$^{-1}$ by Jones et al. (26). A greater variation was also found in the comparison of skin between our calculated mean value of 0.00813 mGy MBq$^{-1}$ and the reported value of 0.0011 mGy MBq$^{-1}$, and between our calculated mean value of 0.01 mGy MBq$^{-1}$ for breast and the reported value of 0.0733 mGy MBq$^{-1}$ (29). For the remaining target organs all reference values are within or close to our calculated uncertainty range.

The dose coefficient uncertainties of $^{99m}$Tc-pertechnetate and $^{99m}$Tc-MAA were also compared to the values reported by ICRP (*1,11*). For $^{99m}$Tc-pertechnetate the reported values for breast, liver, lungs, kidneys, spleen and thymus are within our calculated uncertainty range. For all other target organs, there is a greater deviation of the reported values from our calculated dose coefficient values.

For $^{99m}$Tc-phosphonates, except for red bone marrow, testes and kidneys, other organ dose coefficients reported by ICRP (*1,11*) and Subramanian (*30*) are within our calculated uncertainty range. For $^{99m}$Tc-sestamibi, only the values of gallbladder wall reported by

ICRP (*11*), Higley et al. (*31*) and Wackers et al. (*32*), are in our calculated uncertainty range. Dose coefficients for breast, liver, red bone marrow, stomach wall and thymus are in good agreement with values reported in (*32*). For the remaining target organs, there are greater deviations between the reported values and our calculated uncertainty ranges.

For $^{99m}$Tc-tetrofosmin, absorbed dose coefficients reported by ICRP (*11*) and Higley et al. (*31*) are comparable to our calculated values; however, there is greater deviation for brain and breast. The absorbed dose coefficients reported for liver, spleen, thymus and R-marrow are in the range of the present calculated uncertainty.

For $^{201}$Tl-chloride, absorbed dose coefficients reported by ICRP (*1,11,12*) and by other groups like Thomas et al. (*33*), Castronovo et al. (*34*), Krahwinkel et al. (*35*) and Higley et al. (*31*), are compared to our calculated values. The coefficients for organs of red marrow, kidneys, SI wall and spleen in reference (*35*) are consistent with our calculated values. For other organs, values reported in (*35*) are lower compared to the range of calculated uncertainty and the values reported by other investigators (*1,11,12,33-35*) are greater.

The absorbed dose coefficients reported by ICRP are often not in the calculated uncertainty range. This is because the ICRP used the S values which were derived from the mathematical phantom. These S values often differ greatly from those used in the present calculation. The influence of the S values on the absorbed dose of $^{18}$F-FDG was shown in table 2. The significant difference was found in UB cont. In the mathematical phantom, the SAFs for electrons were not explicitly simulated, but approximated according to the formula (Eq. 8). Zankl et al. (*17*) showed that, by using different mathematical and voxel phantoms, the difference in the dose calculation can be greater than 150 %.

The reference effective dose coefficients reported by ICRP (*1,11,12*) were compared to our calculated values. With the exception of $^{18}$F-FDG, all ICRP reference values are higher than the calculated values and lay outside of the uncertainty range. The uncertainty of tissue-weighting factor was not taken into account as calculating the uncertainty of effective dose coefficients. However, an example of calculation using tissue-weighting factors with a coefficient of variation of 20% showed no significant effect of uncertainty of

284 tissue-weighting factor on uncertainty of effective dose coefficient. The coefficient of
285 variation varies less than 1%.

286 In addition to the theoretical analysis, the patient count rate in SPECT and PET are, in
287 clinical practice, subject to a large uncertainty, and this uncertainty of count rate
288 propagates to the time-integrated activities and will thus affect the overall uncertainties
289 of the dose estimates.

## CONCLUSION

In the present work, a general method was developed for calculating the uncertainty of absorbed dose and effective dose coefficients of seven radiopharmaceuticals commonly used in nuclear medicine. The uncertainties for organ absorbed doses are in the range of 1.1 to 3.3 and for effective dose in the range of 1.1 to 1.4. The urinary bladder wall is the tissue which most commonly shows the highest degree of uncertainty. Furthermore, the uncertainty information can be used to identify the most influential model parameter so that scientific efforts can be invested for updating the pharmacokinetic models and consequently reducing the uncertainty of absorbed dose.

**ACKNOWLEDGEMENT**

This work was financially supported by the German Federal Ministry for the Environment, Nature Conservation, Building and Nuclear Safety (BMUB) under the Contract No. 3612S20013. The authors thank Mr. Randolph Caldwell for the English improvement of the manuscript.

## CONFLICT OF INTEREST

The authors declare that they have no conflict of interest.

**REFERENCES**

**1.** ICRP. *Radiation dose to patients from radiopharmaceuticals.* Oxford, UK: Pergamon Press; 1987. ICRP Publication 53.

**2.** Loevinger R, Budinger T, Watson E. *MIRD primer for absorbed dose calculations. Revised ed.* New York, NY: Society of Nuclear Medicine; 1991;1-21.

**3.** Bolch WE, Eckerman KF, Sgouros G, Thomas SR. MIRD Pamphlet No. 21: A generalized schema for radiopharmaceutical dosimetry - standardization of nomenclature. *J Nucl Med.* 2009;50:477-484.

**4.** Berman M. *MIRD Pamphlet No. 12: Kinetic models for absorbed dose calculations.* New York, NY: Society of Nuclear Medicine; 1976;1-14.

**5.** ICRP. *Adult reference computational phantoms.* Oxford, UK: International Commission on Radiological Protection; 2009. ICRP Publication 110.

**6.** Stabin MG. Radiopharmaceuticals for nuclear cardiology: Radiation dosimetry, uncertainties, and risk. *J Nucl Med.* 2008;49:1555-1563.

**7.** Stabin MG. Uncertainties in internal dose calculations for radiopharmaceuticals. *J Nucl Med.* 2008;49:853-860.

**8.** NCRP. *Uncertainty in internal radiation dose assessment.* Bethesda, MD: National Council on Radiation Protection & Measurement; 2009. NCRP Report 164.

**9.** ICRP. *The 2007 Recommendations of the International Commission on Radiological Protection.* Oxford, UK: Elsevier; 2007. ICRP Publication 103.

**10.** ICRP. *1990 Recommendations of the International Commission on Radiological Protection.* Oxford, UK: Pergamon Press; 1991. ICRP Publication 60.

**11.** ICRP. *Radiation dose to patients from radiopharmaceuticals.* Oxford, UK: Pergamon Press; 1998. ICRP Publication 80.

**12.** ICRP. *Radiation dose to patients from radiopharmaceuticals.* Oxford, UK: International Commission of Radiological Protection; 2008. ICRP Publication 106.

**13.** Iman RL, Shortencarier MJ. *A FORTRAN 77 program and user's guide for the generation of latin hypercube and random samples for use with computer models," NUREGKR-3624 (SAND83-2365)* 1984.

**14.** Hays MT, Segall GM. A mathematical model for the distribution of fluorodeoxyglucose in humans. *J Nucl Med.* 1998;40:1358-1366.

**15.** Li WB, Hoeschen C. Uncertainty and sensitivity analysis of biokinetic models for radiopharmaceuticals used in nuclear medicine. *Radiat Prot Dosim.* 2010;139:228-231.

**16.** Limpert ES, W.E.; Abbt, M. Log-normal distributions across the sciences: keys and clues. *Bioscience.* 2001;51:341-352.

**17.** Zankl M, Schlattl H, Petoussi-Henss N, Hoeschen C. Electron specific absorbed fractions for the adult male and female ICRP/ICRU reference computational phantoms. *Phys Med Biol.* 2012;57:4501-4526.

**18.** ICRP. *Nuclear decay data for dosimetric calculations.* Oxford, UK: International Commission of Radiological Protection; 2008. ICRP Publication 107.

**19.** ICRP. *Limits for intakes of radionuclides by workers. Part 1.* Oxford, UK: Pergamon Press; 1979. ICRP Publication 30.

**20.** Snyder WS, Ford MR, Warner GG. *Estimates of specific absorbed fractions for monoenergetic photon sources uniformly distributed in various organs of a heterogeneous phantom.* New York, NY: Society of Nuclear Medicine; 1978. 5, Revised.

**21.** Leggett RW. Reliability of the ICRP's dose coefficients for members of the public. 1. Sources of uncertainty in the biokinetic models. *Radiat Prot Dosim.* 2001;95:199-213.

**22.** Hays MT, Watson EE, Thomas SR, Stabin MG. MIRD dose estimate report No. 19: Radiation absorbed dose estimates from 18F-FDG. *J Nucl Med.* 2002;43:210-214.

**23.** Mejia AA, Nakamura T, Masatoshi I, Hatazawa J, Masaki M, Watanuki S. Estimation of absorbed doses in humans due to intravenous administration of fluorine-18-fluorodeoxyglucose in PET studies. *J Nucl Med.* 1991;32:699-706.

**24.** Brownell GL, Ackerman RH, Strauss HW, et al. Preliminary imaging results with 18F-2-fluoro-2-deoxy-D-glucose. *J Comput Assist Tomogr.* 1980;4:473-477.

**25.** Reivich M, Kuhl DE, Wolf A, et al. The [18F]fluorodeoxyglucose method for the measurement of local cerebral glucose utilization in man. *Circ Res.* 1979;44:127-137.

**26.** Jones SC, Alavi A, Christman D, Montanez I, Wolf AP, Reivich M. The radiation dosimetry of 2-[F-18]fluoro-2-deoxy-D-glucose in man. *J Nucl Med.* 1982;23:613-617.

**27.** Deloar HM, Fujiwara T, Shidahara M, et al. Estimation of absorbed dose for 2-[F-18]fluoro-2-deoxy-D-glucose using whole-body positron emission tomography and magnetic resonance imaging. *Eur J Nucl Med.* 1998;25:565-574.

**28.** Deloar HM, Fujiwara T, Shidahara M, Nakamura T, Yamadera A, Itoh M. Internal absorbed dose estimation by a TLD method for 18F-FDG and comparison with the dose estimates from whole body PET. *Phys Med Biol.* 1999;44:595-606.

**29.** Khamwan K, Krisanachinda A, Pasawang P. The determination of patient dose from 18F-FDG PET/CT examination. *Radiat Prot Dosim.* 2010;141:50-55.

**30.** Subramanian G, McAfee JG, Blair RJ, Kallfelz FA, Thomas FD. Technetium-99m-methylene diphosphonate - a superior agent for skeletal imaging: comparison with other technetium complexes. *J Nucl Med.* 1975;16:744-755.

**31.** Higley B, Smith FW, Smith T, et al. Technetium-99m-1,2-bis[bis(2-ethoxyethyl) phosphino]ethane: human biodistribution, dosimetry and safety of a new myocardial perfusion imaging agent. *J Nucl Med.* 1993;34:30-38.

**32.** Wackers FJT, Berman DS, Maddahi J, et al. Technetium-99m hexakis 2-methoxyisobutyl isonitrile: human biodistribution, dosimetry, safety, and preliminary comparison to Thallium-201 for myocardial perfusion imaging. *J Nucl Med.* 1989;30:301-311.

**33.** Thomas SR, Stabin MG, Castronovo FP. Radiation-absorbed dose from 201Tl-thallous chloride. *J Nucl Med.* 2005;46:502-508.

**34.** Castronovo FP. 201Tl-labelled TlCl dosimetry revisited. *Nucl Med Commun.* 1993;14:104-107.

**35.** Krahwinkel W, Herzog H, Feinendegen LE. Pharmacokinetics of Thallium-201 in normal individuals after routine myocardial scintigraphy. *J Nucl Med.* 1988;29:1582-1586.

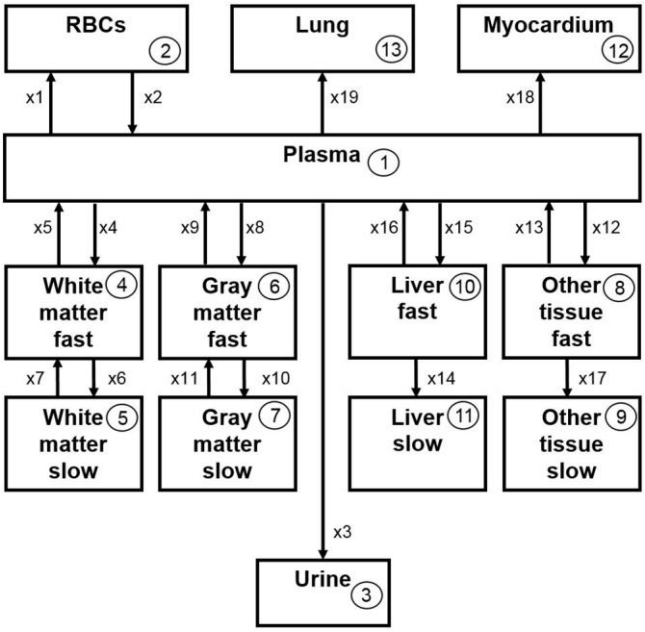


FIGURE 1. Compartmental model for $^{18}$F-FDG developed by MIRD Committee (*14*). RBCs are red blood cells.

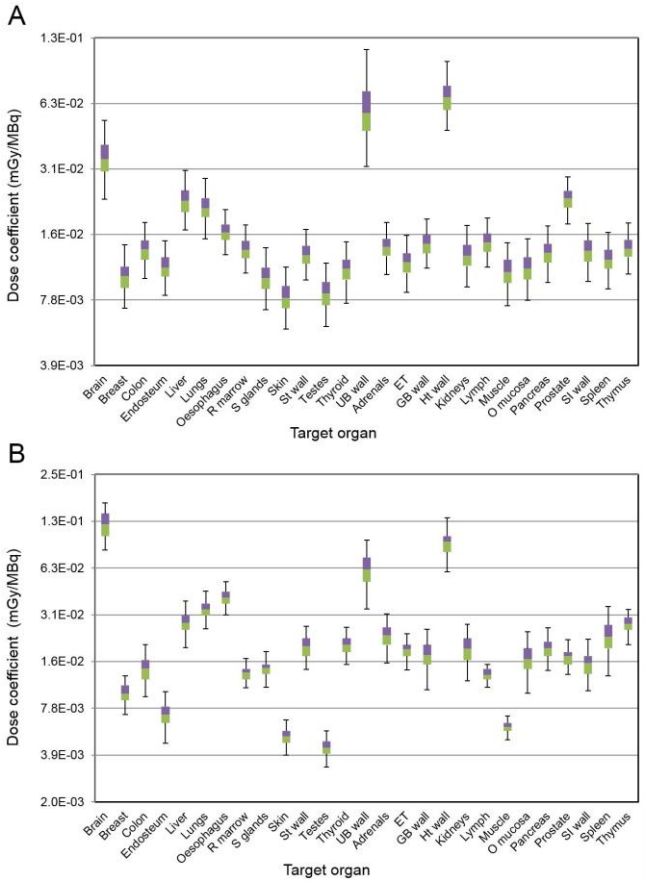


433

434 FIGURE 2. Dose coefficient for $^{18}$F-FDG. According to (A) the ICRP schema and to

435 (B) the MIRD schema.

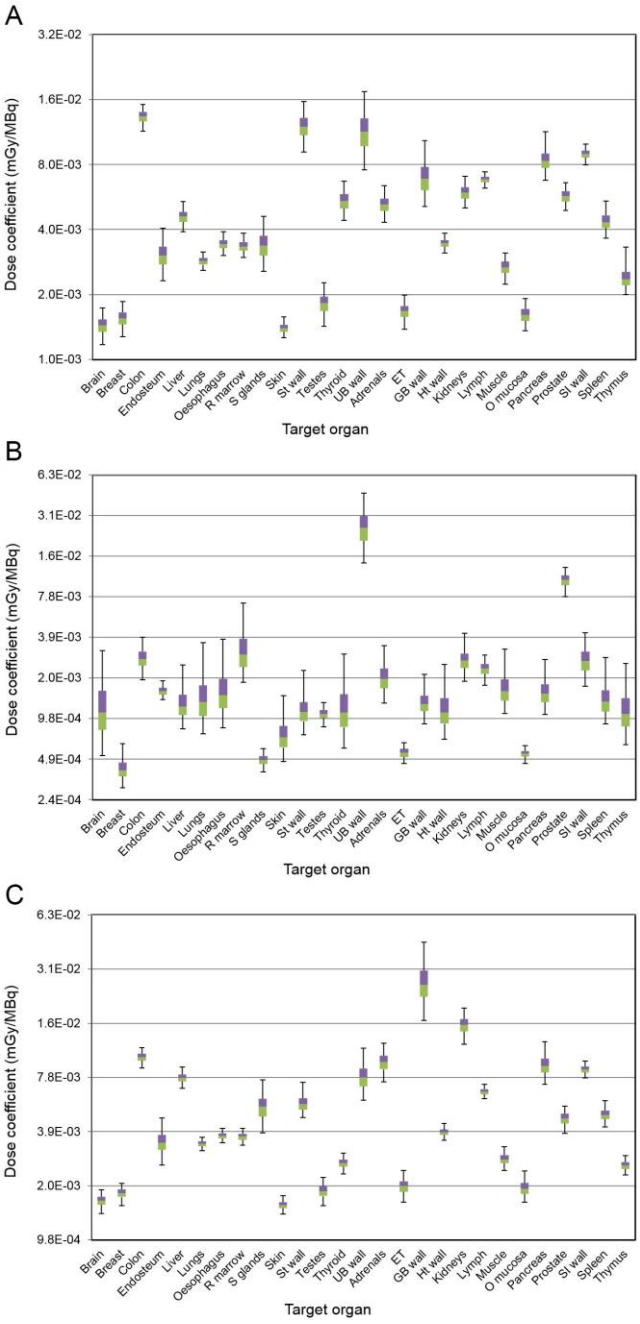


436

437 FIGURE 3. Dose coefficient for (A) $^{99m}$Tc-pertechnetate, (B) $^{99m}$Tc-phosphonate

438 and (C) $^{99m}$Tc-sestamibi. According to the ICRP schema.

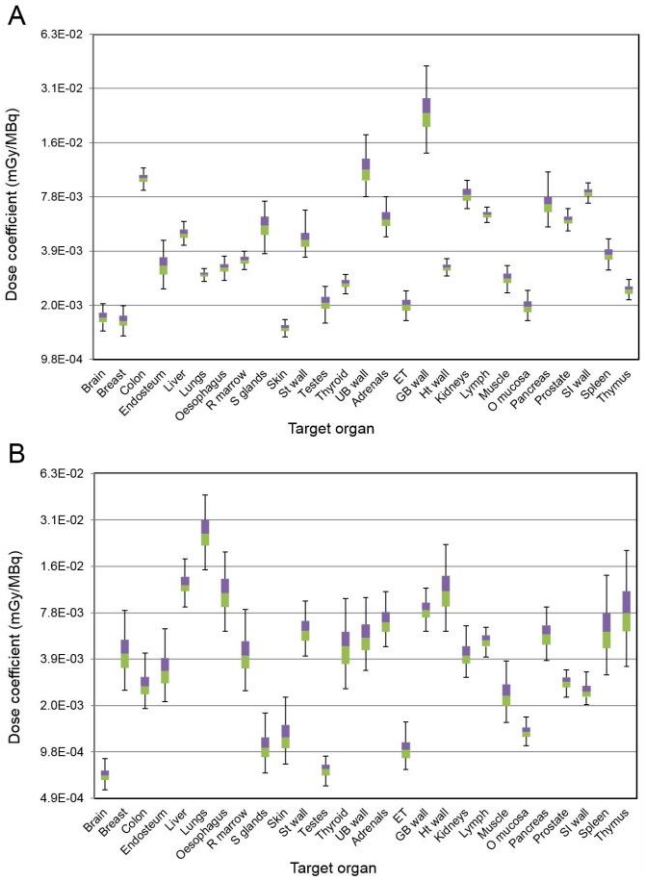


439

440 FIGURE 4. Dose coefficient for (A) $^{99m}$Tc-tetrofosmin and (B) $^{99m}$Tc-MAA.

441 According to the ICRP schema.

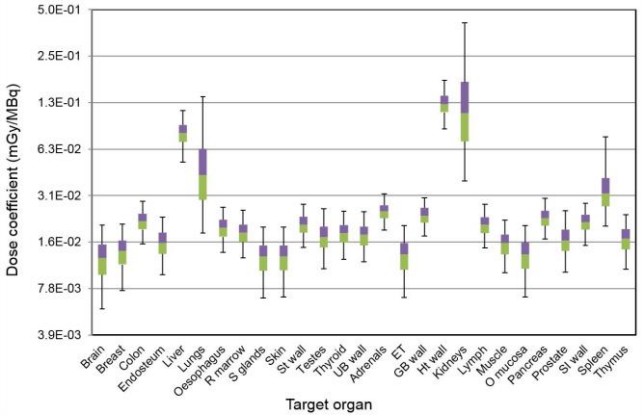


442

443 FIGURE 5. Dose coefficient for $^{201}$Tl-chloride. According to the ICRP schema.

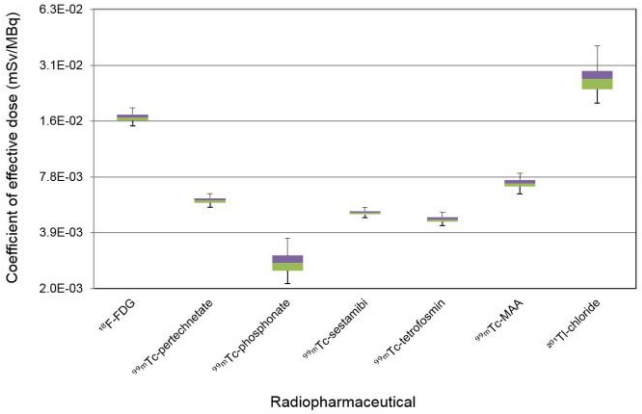


444

445 FIGURE 6. Effective dose coefficients. According to the ICRP schema.

446 **Tables**

447 TABLE 1

448 Phantom Data

| Phantom Name | RCP-AM | RCP-AF | Frank | Golem | MadPat | VisHum | Voxelman |
|---|---|---|---|---|---|---|---|
| Gender | m | f | m | m | m | m | m |
| Age | 38 | 43 | 48 | 38 | 69 | 38 | |
| Height (cm) | 176 | 167 | 174 | 176 | 172 | 180 | 178 |
| Weight (kg) | 73 | 60 | 95 | 69 | 70 | 103 | 70 |
| Number of voxels (mill.) | 1,9 | 3,9 | 23,7 | 1,9 | 6,9 | 20,1 | |
| Coverage | Whole body | Whole body | Head and trunk | Whole body | Head to thigh | Head to thigh | Head to thigh |

449

450 TABLE 2

451 Deviations in absorbed dose calculation for the reference voxel phantoms

452 and mathematical phantoms for $^{18}$F-FDG.

| Target | Voxel Phantom Male | Math. Phantom Male | Voxel Phantom Female | Math. Phantom Female | Male Phantom Voxel/ Math. | Female Phantom Voxel/ Math. |
|---|---|---|---|---|---|---|
| Brain | 3.5E-02 | 3.8E-02 | 3.9E-02 | 4.4E-02 | 8.5% | 13.0% |
| Breast | 9.1E-03 | 9.2E-03 | 1.2E-02 | 1.1E-02 | 1.6% | 5.4% |
| Colon | 1.2E-02 | 1.3E-02 | 1.5E-02 | 1.5E-02 | 6.7% | 2.4% |
| Liver | 2.2E-02 | 2.2E-02 | 2.7E-02 | 2.8E-02 | 0.1% | 3.8% |
| Lungs | 2.0E-02 | 2.0E-02 | 2.4E-02 | 2.5E-02 | 0.4% | 3.6% |
| R-marrow | 1.2E-02 | 1.2E-02 | 1.4E-02 | 1.4E-02 | 6.4% | 4.2% |
| Skin | 7.3E-03 | 8.3E-03 | 8.7E-03 | 9.7E-03 | 13.8% | 11.6% |
| St wall | 1.2E-02 | 1.1E-02 | 1.4E-02 | 1.3E-02 | 10.7% | 3.1% |
| Thyroid | 1.0E-02 | 1.1E-02 | 1.2E-02 | 1.3E-02 | 8.6% | 7.7% |
| UB wall | 6.9E-02 | 2.2E-01 | 1.0E-01 | 2.8E-01 | 212.8% | 184.8% |
| Adrenals | 1.3E-02 | 1.3E-02 | 1.6E-02 | 1.5E-02 | 0.4% | 2.0% |
| ET | 1.0E-02 | 1.1E-02 | 1.2E-02 | 1.3E-02 | 3.9% | 3.7% |
| GB wall | 1.4E-02 | 1.3E-02 | 1.6E-02 | 1.5E-02 | 7.9% | 7.6% |
| Ht wall | 6.2E-02 | 6.7E-02 | 7.9E-02 | 8.9E-02 | 7.2% | 12.2% |
| Kidneys | 1.2E-02 | 1.1E-02 | 1.4E-02 | 1.4E-02 | 3.1% | 0.9% |
| Muscle | 9.5E-03 | 1.1E-02 | 1.1E-02 | 1.3E-02 | 14.4% | 12.1% |
| Pancreas | 1.3E-02 | 1.3E-02 | 1.4E-02 | 1.6E-02 | 2.6% | 14.2% |
| SI wall | 1.3E-02 | 1.2E-02 | 1.6E-02 | 1.5E-02 | 5.2% | 6.9% |
| Spleen | 1.2E-02 | 1.1E-02 | 1.3E-02 | 1.4E-02 | 4.0% | 1.8% |
| Thymus | 1.2E-02 | 1.2E-02 | 1.6E-02 | 1.4E-02 | 3.2% | 7.5% |

453